

Discovery of 4-Piperazine Isoquinoline Derivatives as Potent and Brain-Permeable Tau Prion Inhibitors with CDK8 Activity

Jean-Marc M. Grandjean, Alexander Y. Jiu, John W. West, Atsushi Aoyagi, Daniel G. Droege, Manuel Elepano, Makoto Hirasawa, Masakazu Hirouchi, Ryo Murakami, Joanne Lee, Koji Sasaki, Shimpei Hirano, Takao Ohyama, Benjamin C. Tang, Roy J. Vaz, Masahiro Inoue, Steven H. Olson, Stanley B. Prusiner, Jay Conrad,* and Nick A. Paras



Cite This: <https://dx.doi.org/10.1021/acsmmedchemlett.9b00480>



Read Online

ACCESS |



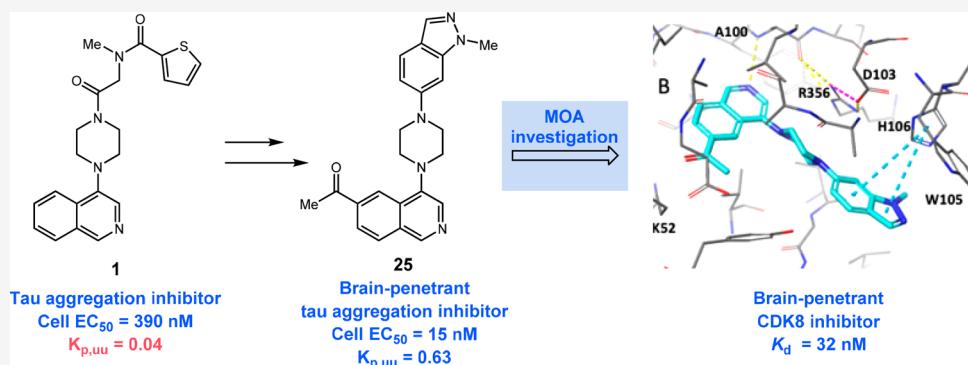
Metrics & More



Article Recommendations



Supporting Information



ABSTRACT: Tau prions feature in the brains of patients suffering from Alzheimer's disease and other tauopathies. For the development of therapeutics that target the replication of tau prions, a high-content, fluorescence-based cell assay was developed. Using this high-content phenotypic screen for nascent tau prion formation, a 4-piperazine isoquinoline compound (**1**) was identified as a hit with an EC_{50} value of 390 nM and 0.04 $K_{p,uu}$. Analogs were synthesized using a hypothesis-based approach to improve potency and *in vivo* brain penetration resulting in compound **25** (EC_{50} = 15 nM; $K_{p,uu}$ = 0.63). We investigated the mechanism of action of this series and found that a small set of active compounds were also CDK8 inhibitors.

KEYWORDS: Tau, neurodegeneration, phenotypic assay, prion, CDK8, brain permeation

Aggregation of the tau protein in the CNS is a pathological hallmark of neurodegenerative diseases that include Alzheimer's disease, chronic traumatic encephalopathy, corticobasal degeneration, and progressive supranuclear palsy, among others.¹ These diseases, collectively known as tauopathies, are caused by tau prions that induce templated misfolding of unstructured tau and its subsequent spread throughout the brain.^{2,3} Thus, therapeutic agents that slow the spread of tau prions in the brain or clear tau prion aggregates may constitute an effective strategy for the discovery of disease-altering treatments for tauopathy patients.

Over the past few years, our group and others have developed cell assays to model tau propagation using cell lines that express mutant human tau linked to YFP.^{4,5} When these cells are exposed to patient-derived tau, cellular tau undergoes templated misfolding, which induces the formation of fluorescent puncta. We hypothesized that this concept could provide the basis for a phenotypic high-content screen. To match the tau isoform expressed in the Tg2541^{+/+} mouse model,⁶ we created a HEK 293T cell line expressing human

0N4R(P301S)Tau-YFP. Using this cell line, we posited that hit compounds that prevented or slowed formation of nascent 0N4R(P301S)Tau-YFP puncta in T24(S) HEK cells was used as the starting point for a drug discovery program for tauopathy.

Compound **1** was identified from a phenotypic high-content screening campaign in T24(S) HEK cells (Figure 1). This compound possessed good initial potency with an EC_{50} value of 390 nM but low stability in mouse microsomes (2% of parent remaining after 30 min incubation). Other ADME parameters were encouraging; **1** showed high *in vitro* permeability (P_{A-B} = 53.2×10^{-6} cm/s) with a low efflux ratio (ER = 1.7)⁷ in LLC PK (mdr1) cells, and its calculated physicochemical properties led to a high CNS MPO^{8,9} score of

Received: October 17, 2019

Accepted: January 14, 2020

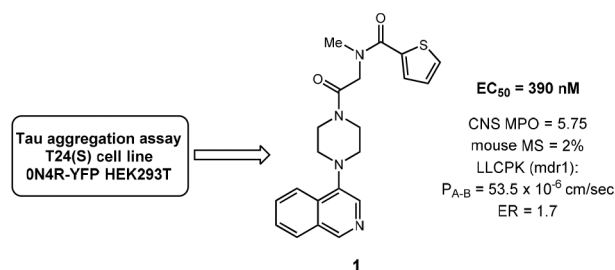


Figure 1. High-content screening hit in T24(S) cells.

5.75 out of 6. The latter finding suggests that **1** might be brain-penetrant *in vivo*.

To determine the baseline brain permeability for compounds in this series, **1** was dosed orally in B6/J mice, and their brains were collected after 2 h. Despite its low LLCPK (mdr1) efflux ratio and high CNS MPO score, a low unbound brain/blood partition constant ($K_{p,uu} = 0.04$) was observed for **1** *in vivo*, indicating that it was a likely substrate for efflux transporters (Table 1). Given the discrepancy between *in vitro*

Table 1. Polar Group Effect on $K_{p,uu}$

compound	EC ₅₀ (μM)	C _{plasma} (μM)	C _{brain} (μM)	K _p ^a	K _{p,uu}
1	0.39	2.8 ^b	0.2 ^b	0.07	0.04
2	0.91	1.0 ^c	0.4 ^c	0.4	0.2
3	>10.0	1.5 ^c	1.2 ^c	0.8	0.4

^aB6/J mice, 10 mg/kg (gavage, 0.5% MC). ^bPlasma and brain concentrations at 0.5 h post administration. ^cPlasma and brain concentrations at 1 h post administration.

ER and *in vivo* K_p observed for **1**, further optimization was guided by *in vivo* K_p . To better understand how polar moieties interact with transporters to recognize **1**, we synthesized compounds **2** and **3**, wherein either the thiophene amide or the isoquinoline nitrogen were removed. Improved *in vivo* unbound partition coefficients were observed for the compounds (**2**, $K_{p,uu} = 0.2$; **3**, $K_{p,uu} = 0.4$), suggesting that the high hydrogen-bond avidity of both moieties¹⁰ could contribute to transporter recognition. With two potential avenues to reduce efflux, we decided to focus on thiophene amide replacement rather than isoquinoline modification. Compared with compound **1**, **2** greatly improved $K_{p,uu}$ combined with reduced molecular weight (**2**, 297 g/mol; **1**, 394 g/mol), while only sacrificing about 2-fold in cell potency (**1**, EC₅₀ = 0.39 μM; **2**, EC₅₀ = 0.90 μM).

Our initial strategy for improving the activity of **2** began by replacing the *tert*-butyl with a heteroatom containing substituents on the piperazine amide (Table 2). We were encouraged by tetrahydrofuran **4** and oxetane **5**, which retained activity while maintaining acceptable metabolic stability. Substituted pyrazoles, oxazoles, and thiazoles were synthesized to survey activity and metabolic stability of

Table 2. Amide Replacement: Effect on EC₅₀ and MS

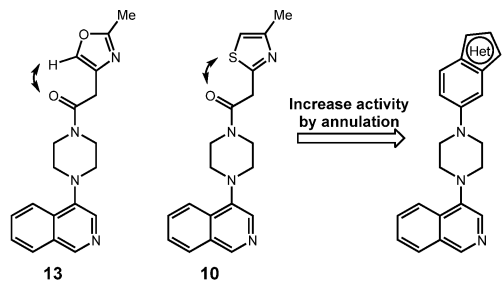
R	EC ₅₀ (μM)	MS (%) ^a	R	EC ₅₀ (μM)	MS (%) ^a
4	0.59	63	10	0.12	13
5	1.42	57	11	0.40	1
6	>10	21	12	>10	76
7	>10	66	13	0.28	64
8	0.52	46	14	0.12	18
9	0.17	1	15	0.68	1

^a% remaining after 30 min incubation with mouse microsomes.

heterocycles. Isomeric pyrazoles **7** and **8** showed vastly different cell activity, indicating that heterocycles are tolerated but the position of the methyl substituent is critical. Additionally, replacing methyl (**8**) with isopropyl (**9**) further improved activity. Compound **9** was the first analog generated with potency (EC₅₀ = 170 nM) greater than compound **1**, although metabolic stability was greatly reduced (MS = 1%). Thiazole-bearing compounds **10** and **11** were also active but suffered from diminished metabolic stability (**10**, MS = 13%; **11**, MS = 1%). Oxazoles **13** and **14** confirmed the trend observed for **8** and **9**, where a methyl to cyclopropyl change affords an improvement in EC₅₀, while expansion to a *tert*-butyl decreased activity (**15**). However, despite the advances in activity and metabolic stability observed for selected compounds in Table 2, we still desired additional improvements in EC₅₀.

To improve the inhibition of tau prion activity, we adopted a rigidification strategy for the series. The calculated low energy conformations¹¹ of the most potent methyl-substituted compounds, **10** and **13**, have the piperazine-amide carbonyl in the plane with the heterocycle due to either a weak hydrogen bond between the carbonyl oxygen and the heterocycle¹² in **13** or a noncovalent interaction between oxygen and the thiazole sulfur¹³ in **10** (Table 2). If the conformations favoring these putative intramolecular interactions were responsible for the enhanced activity of these compounds, replacing the amide with a [6,5]-fused heterocycle should lead to improvements in activity (Table 3). This strategy was particularly successful in the case of indazole **18**, which had an EC₅₀ of 22 nM and maintained acceptable microsomal stability (MS = 46%). Interestingly, regioisomer **21** was more than five times less active than **18** while benzoxazoles **16** and **17** were inactive despite the comparable activities of oxazoles and pyrazoles in Table 2. Pyridoimidazole **22** and pyrido-pyrrole **23** were less active than the indazoles, and both analogs of **18**, compounds **19** and **20**, bearing either a 7-N or 7-C-F were inactive in the assay, indicating that stereoelectronic factors may influence activity.

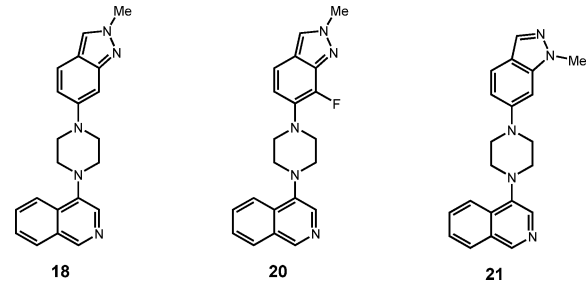
Table 3. Rigidification Strategy to Improve Activity



	R	EC ₅₀ (μM)	MS (%) ^a		R	EC ₅₀ (μM)	MS (%) ^a
16		>10	65	20		>10	56
17		>10	50	21		0.12	64
18		0.022	46	22		1.1	88
19		>10	60	23		0.33	1

^a% remaining after 30 min incubation with mouse microsomes.

Compound 18 was tested in a mouse PK experiment to determine its K_p at 2 h post administration (Table 4). Despite

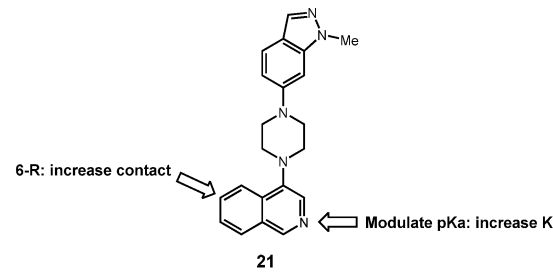
Table 4. Effect of [6,5]-Fused Rings on $K_{p,uu}$


	T24(S)	EC ₅₀ (μM)	C _{plasma} ^a (μM)	C _{brain} ^a (μM)	K_p	$K_{p,uu}$
18		0.022	11.4	0.15	0.01	0.005
20		>10	3.2	3.9	1.2	0.53
21		0.12	9.0	6.80	0.75	0.35

^aB6/J mice, plasma, and brain concentrations at 2 h post administration, 10 mg/kg (gavage, 0.5% MC).

its low PSA (37.2 Å²) and deletion of the tertiary amide, 18 showed poor brain exposure in mice (K_p = 0.01; $K_{p,uu}$ = 0.05), much lower than that observed for 2. Although less active than 18, compounds 20 and 21 were tested *in vivo* to determine the factors governing efflux for indazole derivatives. Compound 20 was chosen to assess whether fluorination and subsequent lowering of indazole pK_a could improve brain penetration. Conversely, 21 was identified as an active analog where the directionality of the basic nitrogen and the methyl substituent were modified relative to 18, in an attempt to disrupt recognition by efflux transporters. Both 20 and 21 had significantly improved unbound brain/blood ratios (20, $K_{p,uu}$ = 0.53; 21, $K_{p,uu}$ = 0.35), indicating the importance of the indazole stereoelectronics in transporter recognition. Given that 21 was still active in the tau prion bioassay (EC₅₀ = 120 nM), we focused on improving the potency of this compound.

The increased $K_{p,uu}$ achieved with 3 suggested that reducing the isoquinoline pK_a would lead to improved brain exposure. As summarized in Table 5, we observed that the introduction

Table 5. Strategy to Increase Activity and $K_{p,uu}$


	R	EC ₅₀ (μM)	MS (%) ^a	C _{plasma} ^b (μM)	C _{brain} ^b (μM)	K_p	$K_{p,uu}$
24		>10					
25		0.015	12	1.7	1.6	0.95	0.63
26		0.035	34	1.9	3.5	1.85	0.56
27		0.098	47	4.3	5.1	1.23	0.34

^a% remaining after 30 min incubation with mouse microsomes. ^bB6/J mice, plasma, and brain concentrations at 2 h post administration, 10 mg/kg (gavage, 0.5% MC).

of electron-withdrawing substituents at the isoquinoline 6-position was well-tolerated in the assay. In particular, 25 and 26 with hydrogen-bond acceptors were very active tau aggregation inhibitors (EC₅₀ (25) = 15 nM; EC₅₀ (26) = 35 nM). Furthermore 25, 26, and 27 achieved high unbound brain/blood partition coefficients. It is possible that any negative contribution toward efflux caused by these polar substituents was offset by the concomitant reduction of isoquinoline pK_a . In any event, compounds 25 and 26 became our new benchmarks with high potency and good brain exposure.

As a first step toward elucidating the mechanism of action of compounds in this series, we engaged in a literature similarity search. In particular, our search focused on biologically active substituted quinolines bearing cyclic moieties at the 4-position. We quickly identified BI-1347^{14,15} (labeled 28), a potent CDK8/cyclinC¹⁶ inhibitor discovered by Boehringer Ingelheim, with a reported *in vitro* IC₅₀ of 1 nM. We were struck by the resemblance between 28 and the 4-piperazine-substituted isoquinolines described in Figure 2. We tested BI-1347 in the T24(S) cell assay and found it to be a potent tau aggregation inhibitor with an EC₅₀ of 5 nM. To assess whether CDK8 was a potential target for compounds in our series, we selected three analogs with differing cell EC₅₀s for CDK8 K_d determination. Comparing intrinsic EC₅₀ in the tau aggregation assay (cell assay activities corrected for free fraction in medium) and CDK8 K_d , we found that more active tau aggregation inhibitors had lower CDK8 K_d (Table 6). Published data for BI-1347¹⁴ indicated that it is selective for CDK8 and its paralog CDK19 over other kinases, and a screen for 25 (included in the S11) showed that it is selective for CDK8/19 over 468 kinases tested except for PI4KB.

Compounds 28, 25, 21, and 13 (along with 29,¹⁷ a CDK8 inhibitor (IC₅₀ of 0.9 nM; EC₅₀ of 9 nM in the T24(S) assay)

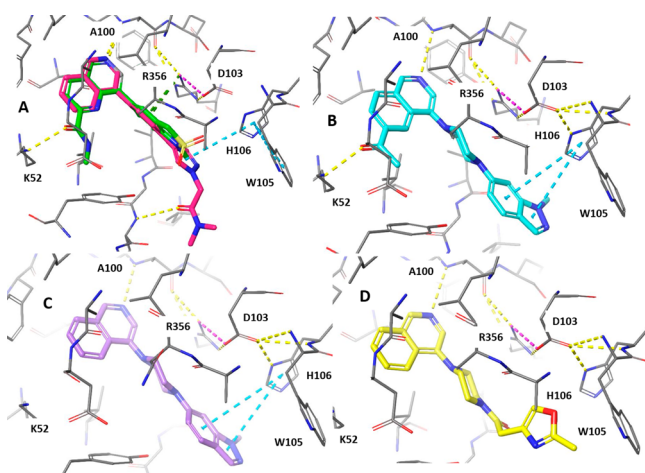


Figure 2. Docking to CDK8 crystal structure. (A) **28** and **29**, (B) **25**, (C) **21**, and (D) **13** docked to SICP.

Table 6. CDK8 Inhibition Relative to BI-1347

	EC ₅₀ (μM)	intEC ₅₀ ^a (nM)	CDK8 K _d (nM)	K _{p,uu} ^b
13	0.22	210	600	0.07
21	0.12	30.0	30.0	0.35
25	0.015	5.0	32.0	0.63
28	0.005	2.0	0.77	0.01

^aEC₅₀ corrected for protein binding in assay medium. ^bDetermined from *in vivo* K_p at 2 h, 10 mg/kg (gavage, 0.5% MC).

of similar structure) were docked to a known cocrystal structure of CDK8¹⁸ and **29** (Figure 2). In accordance with the reported structure,¹⁹ key interactions for binding of **29** were reproduced *in silico*, namely amide binding to Lys52, hinge binding to Ala100, and a cation– π interaction with Arg356. The docked structures of **28** and **29** (Figure 2A) adopt a similar orientation, although **28** extends further and has an additional π – π interaction between its pyrazole ring and His106. Combined, these interactions account for the very low K_d (0.77 nM) observed for this ligand. Compounds **25**, **21**, and **13** were predicted to bind in the same orientation as **28** with the isoquinoline nitrogen interacting with Ala100. Analogous to **29** the methyl ketone of **25** made a hydrogen bond to Lys52. We postulate that the lower activity of **25**, **21**, and **13** compared to the previously published compounds is due to the replacement of phenyl with piperazine and subsequent loss of the cation– π interaction with Arg356. Interestingly, in the case of **25** and **21** the face of the indazole ring makes a close interaction with the edge of His106. These interactions are likely to be strong given the proximity of His106 to Asp103 and Arg356 and the fact that His106 may be partially charged. The oxazole in compound **13** points away from His106 and

cannot engage in this π – π interaction, providing a reasonable explanation for its higher K_d (600 nM).

Given the activity of BI-1347 as an inhibitor of tau aggregation, it was tested in *in vivo* K_p and found to distribute poorly to the brain (K_{p,uu} = 0.01) (Table 6). On the other hand, **21** and **25** are potent CDK8 inhibitors capable of crossing the BBB (K_{p,uu}(**21**) = 0.35 and K_{p,uu}(**25**) = 0.63). To the best of our knowledge, these are the first examples of CDK8 inhibitors with *in vivo* BBB permeability and low efflux. The correlation between CDK8 inhibition and tau aggregation inhibition is under further investigation. However, the discovery of brain-penetrant CDK8 inhibitors could be of interest to the oncology community.

In summary, we optimized a series of 4-piperazine isoquinoline compounds that inhibit tau prion activity. SAR studies were guided by optimization of compound activity and improvements to *in vivo* brain exposure in mice. Improvements to K_{p,uu} were achieved through rational design and key experiments to identify the structural elements responsible for high BBB efflux. A similarity search identified the CDK8 inhibitor BI-1347 as a potent tau prion inhibitor in our T24(S) cell assay. Compounds from the 4-piperazine isoquinoline series were found to be potent, brain-penetrant CDK8 inhibitors, and their binding to CDK8 was further supported by docking studies. Efforts toward the optimization of these tau prion inhibitors are ongoing.

■ ASSOCIATED CONTENT

Supporting Information

The Supporting Information is available free of charge at <https://pubs.acs.org/doi/10.1021/acsmchemlett.9b00480>.

Experimental procedures for compound synthesis and characterization, biological assays, computation methods, and kinase selectivity data for compound **25** (PDF)

■ AUTHOR INFORMATION

Corresponding Author

Jay Conrad – Institute for Neurodegenerative Diseases (IND), UCSF Weill Institute for Neurosciences, University of California, San Francisco, San Francisco, California 94518, United States; orcid.org/0000-0002-9048-8833; Email: jay.conrad@ucsf.edu

Authors

Jean-Marc M. Grandjean – Institute for Neurodegenerative Diseases (IND), UCSF Weill Institute for Neurosciences, University of California, San Francisco, San Francisco, California 94518, United States

Alexander Y. Jiu – Institute for Neurodegenerative Diseases (IND), UCSF Weill Institute for Neurosciences, University of California, San Francisco, San Francisco, California 94518, United States

John W. West – Institute for Neurodegenerative Diseases (IND), UCSF Weill Institute for Neurosciences, University of California, San Francisco, San Francisco, California 94518, United States

Atsushi Aoyagi – R&D Division, Daiichi Sankyo Co., Ltd., Tokyo 140-8710, Japan

Daniel G. Droege – Institute for Neurodegenerative Diseases (IND), UCSF Weill Institute for Neurosciences, University of California, San Francisco, San Francisco, California 94518, United States

Manuel Elepano – Institute for Neurodegenerative Diseases (IND), UCSF Weill Institute for Neurosciences, University of California, San Francisco, San Francisco, California 94518, United States

Makoto Hirasawa – R&D Division, Daiichi Sankyo Co., Ltd., Tokyo 140-8710, Japan

Masakazu Hirouchi – R&D Division, Daiichi Sankyo Co., Ltd., Tokyo 140-8710, Japan

Ryo Murakami – R&D Division, Daiichi Sankyo Co., Ltd., Tokyo 140-8710, Japan

Joanne Lee – Institute for Neurodegenerative Diseases (IND), UCSF Weill Institute for Neurosciences, University of California, San Francisco, San Francisco, California 94518, United States

Koji Sasaki – R&D Division, Daiichi Sankyo Co., Ltd., Tokyo 140-8710, Japan

Shimpei Hirano – R&D Division, Daiichi Sankyo Co., Ltd., Tokyo 140-8710, Japan

Takao Ohyama – R&D Division, Daiichi Sankyo Co., Ltd., Tokyo 140-8710, Japan

Benjamin C. Tang – Institute for Neurodegenerative Diseases (IND), UCSF Weill Institute for Neurosciences, University of California, San Francisco, San Francisco, California 94518, United States

Roy J. Vaz – Institute for Neurodegenerative Diseases (IND), UCSF Weill Institute for Neurosciences, University of California, San Francisco, San Francisco, California 94518, United States

Masahiro Inoue – R&D Division, Daiichi Sankyo Co., Ltd., Tokyo 140-8710, Japan

Steven H. Olson – Institute for Neurodegenerative Diseases (IND), UCSF Weill Institute for Neurosciences, University of California, San Francisco, San Francisco, California 94518, United States

Stanley B. Prusiner – Institute for Neurodegenerative Diseases (IND), UCSF Weill Institute for Neurosciences, University of California, San Francisco, San Francisco, California 94518, United States

Nick A. Paras – Institute for Neurodegenerative Diseases (IND), UCSF Weill Institute for Neurosciences, University of California, San Francisco, San Francisco, California 94518, United States;
orcid.org/0000-0001-5742-4056

Complete contact information is available at:
<https://pubs.acs.org/10.1021/acsmmedchemlett.9b00480>

Funding

This work was supported by a grant from the National Institutes of Health (AG002132) (S.B.P.), as well as by support from the Brockman Foundation (S.B.P.) and the Sherman Fairchild Foundation (S.B.P.).

Notes

The authors declare the following competing financial interest(s): The Institute for Neurodegenerative Diseases has a research collaboration with Daiichi Sankyo (Tokyo, Japan). Stanley B. Prusiner is a member of the Scientific Advisory Board of ViewPoint Therapeutics and a member of the Board of Directors of Trizell, Ltd., neither of which have contributed financial or any other support to these studies.

ABBREVIATIONS

BBB, blood brain barrier; ER, efflux ratio; CNS MPO, central nervous system multiparameter optimization; HEK, human embryonic kidney; LLC PK, pig kidney cell line; PK,

pharmacokinetics; PSA, polar surface area; SAR, structure activity relationship; YFP, yellow fluorescent protein

REFERENCES

- (1) Goedert, M. Alzheimer's and Parkinson's Diseases: The Prion Concept in Relation to Assembled A β , tau, and α -Synuclein. *Science* **2015**, *349*, 1255555.
- (2) Aoyagi, A.; Condello, C.; Stöhr, J.; Yue, W.; Lee, J. C.; Rivera, B. M.; Woerman, A. L.; Halliday, G.; van Duinen, S.; Ingelsson, M.; Lannfelt, L.; Graff, C.; Bird, T. D.; Keene, C. D.; Seeley, W. W.; DeGrado, W. F.; Prusiner, S. B. A β and tau Prion-like Activities Decline with Longevity in the Alzheimer's Disease Human Brain. *Sci. Transl. Med.* **2019**, *11*, 8462.
- (3) Ayers, J. I.; Giasson, B. I.; Borchelt, D. R. Prion-like Spreading in Tauopathies. *Biol. Psychiatry* **2018**, *83*, 337–346.
- (4) Woerman, A. L.; Aoyagi, A.; Patel, S.; Kazmi, S. A.; Lobach, I.; Grinberg, L. T.; McKee, W. W.; Olson, S. H.; Prusiner, S. B. Tau Prions from Alzheimer's Disease and Chronic Traumatic Encephalopathy Patients Propagate in Cultured Cells. *Proc. Natl. Acad. Sci. U. S. A.* **2016**, *113*, E8187–E8196.
- (5) Sanders, D. W.; Kaufman, S. K.; DeVos, S. L.; Sharma, A. M.; Mirbaha, H.; Barker, S. J.; Foley, A.; Thorpe, J. R.; Serpell, L. C.; Miller, T. M.; Grinberg, L. T.; Seeley, W. W.; Diamond, M. I. Distinct Tau Prion Strains Propagate in Cells and Mice and Define Different Tauopathies. *Neuron* **2014**, *82*, 1271–1288.
- (6) Allen, B.; Ingram, E.; Takao, M.; Smith, M. J.; Jakes, R.; Virdee, K.; Yoshida, H.; Holzer, M.; Craxton, M.; Emson, P. C.; Atzori, C.; Migheli, A.; Crowther, R. A.; Ghetti, B.; Spillantini, M. G.; Goedert, M. Abundant Tau Filaments and Nonapoptotic Neurodegeneration in Transgenic Mice Expressing Human P301S Tau Protein. *J. Neurosci.* **2002**, *22*, 9340–9351.
- (7) Rankovic, Z. CNS Drug Design: Balancing Physicochemical Properties for Optimal Brain Exposure. *J. Med. Chem.* **2015**, *58*, 2584–2608.
- (8) Wager, T. T.; Xinjun, H.; Verhoest, P. R.; Villalobos, A. Moving Beyond Rules: The Development of a Central Nervous System Multiparameter Optimization (CNS MPO) Approach To Enable Alignment of Druglike Properties. *ACS Chem. Neurosci.* **2010**, *1*, 435–449.
- (9) Wager, T. T.; Xinjun, H.; Verhoest, P. R.; Villalobos, A. Central Nervous System Multiparameter Optimization Desirability: Application in Drug Discovery. *ACS Chem. Neurosci.* **2016**, *7*, 767–775.
- (10) Abraham, M. H.; Duce, P. P.; Prior, D. V.; Barratt, D. G.; Morris, J. J.; Taylor, P. J. Hydrogen Bonding. Part 9. Solute Proton Donor and Proton Acceptor Scales for Use in Drug Design. *J. Chem. Soc., Perkin Trans. 2* **1989**, *6*, 699–711.
- (11) Conformational searching was performed using Maestro version 12 available from Schrödinger, LLC, New York, USA.
- (12) Pierce, A. C.; ter Haar, E.; Binch, H. M.; Kay, D. P.; Patel, S. R.; Li, P. CH⁺O and CH⁺N Hydrogen Bonds in Ligand Design: A Novel Quinazolin-4-ylthiazol-2-ylamine Protein Kinase Inhibitor. *J. Med. Chem.* **2005**, *48*, 1278–1281.
- (13) Pascoe, D. J.; Ling, K. B.; Cockroft, S. L. The Origin of Chalcogen Bonds. *J. Am. Chem. Soc.* **2017**, *139*, 15160–15167.
- (14) opnMe (Boehringer Ingelheim). CDK8 Inhibitor BI-1347. <https://opnme.com/molecules/cdk8-bi-1347> (accessed July 16, 2019).
- (15) Engelhardt, H.; Arnhof, H.; Carotta, S.; Hofmann, M. H.; Kerenyi, M.; Scharn, D. New Phenylpyrazolylacetamide Compounds and Derivatives as CDK8/CDK19 Inhibitors. WO2017202719A1, 2017.
- (16) Xi, M.; Chen, T.; Wu, C.; Gao, X.; Wu, Y.; Luo, X.; Du, K.; Yu, L.; Cai, T.; Shen, R.; Sun, H. CDK8 as a Therapeutic Target for Cancers and Recent Developments in Discovery of CDK8 Inhibitors. *Eur. J. Med. Chem.* **2019**, *164*, 77–91.
- (17) Mallinger, A.; Schiemann, K.; Rink, C.; Sejberg, J.; Honey, M. A.; Czodrowski, P.; Stubbs, M.; Poeschke, O.; Michael, B.; Schneider, R.; Schwarz, D.; Musil, D.; Burke, R.; Urbahns, K.; Wienke, D.; Clarke, P. A.; Raynaud, F. I.; Eccles, S. A.; Rohdich, F.; Blagg, J. 2.8-

Disubstituted-1,6-Naphthyridines and 4,6-Disubstituted-Isoquinolines with Potent, Selective Affinity for CDK8/19. *ACS Med. Chem. Lett.* **2016**, 7, 573.

(18) Czodrowski, P.; Mallinger, A.; Wienke, D.; Esdar, C.; Poshke, O.; Busch, M.; Rohdich, F.; Eccles, S. A.; Ortiz-Ruiz, M.-J.; Schneider, R.; Raynaud, F. I.; Clarke, P. A.; Musil, D.; Schwarz, D.; Dale, T.; Urbahns, K.; Blagg, J.; Schiemann, K. Structure-Based Optimization of Potent, Selective, and Orally Bioavailable CDK8 Inhibitors Discovered by High-Throughput Screening. *J. Med. Chem.* **2016**, 59, 9337–9349.

(19) PDB code: 5I5Z.